Film boiling heat transfer from micro heat sinks driven by Bénard-Marangoni convection

Francisco J. Arias[a] and Salvador De Las Heras[a*]
[a] *Department of Fluid Mechanics, Polytechnic University of Catalonia, ESEIAAT C/ Colom 11, 08222 Barcelona, Spain*
(Dated: November 1, 2020)

Bénard-Marangoni convection and its significance with regard to film boiling heat transfer from micro heat sinks is discussed. In recent works cooling performance of micro heat sinks has been studied showing that two-phase cooling could be more efficient than single-phase cooling. However, in those previous works was also found that the critical heat flux (CHF) i.e., the transition from a nucleate boiling regime to an almost insulating film boiling regime was the main limitation of two-phase cooling. Here, it is shown that owing to the induced thermal gradient along the fin and the very small fin-spacing, Bénard-Marangoni convection (which was neither considered nor mentioned so far) can play an important role and in fact driven the entire film boiling heat and mass transfer process. The reason behind this lies in the fact that in film boiling the interfacial vapor-liquid velocity is the capital factor rather than the bulk velocity, and this can be at least one order of magnitude higher from Bénard-Marangoni convection. Utilizing a simplified physical model, an analytical expression for the film boiling heat transfer coefficient driven by Bénard-Marangoni was derived. Computational Fluid Dynamics (CFD) simulations were performed and comparison between natural and Bénard-Marangoni convective heat transfer presented.

Keywords. *Micro heat sinks; Film boiling heat transfer; Microfluidics; Microsystems applications; Bénard-Marangoni convection; Natural convection*

I. INTRODUCTION

Heat transfer in microsystems applications are becoming an important and almost vital topic in current and future human life and society. Electronics miniaturization show no signs of slowing in the near future,[1], and the inherent limitations associated with electronic miniaturization as regard space, translates in the fact that microscale heat removal systems set the ultimate limit in the miniaturization. Microscale natural convection and forced convection single phase has been studied in the past both analytical and computer simulations [2]-[9], as well as two-phase cooling [10]-[12]. It was found that two-phase cooling could be more effective and efficient for micro heat sinks, however, it was also found that the critical heat flux (CHF) i.e., the transition from a nucleate boiling regime to an almost insulating film boiling regime was the main limitation of two-phase cooling,[13]

Nevertheless, in those previous works, Bénard-Marangoni convection was neither considered nor mentioned. Here, it is shown that owing to the induced thermal gradient along the fin and the very small fin-spacing, Bénard-Marangoni convection stars to play an important role and indeed drives the film boiling heat transfer regime.

* Corresponding author: Tel.: +93 73 98 666; francisco.javier.arias@upc.edu

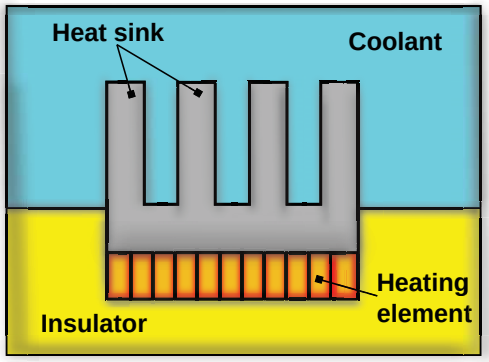

FIG. 1. Vertical heat transfer using a micro heat sinks.

II. METHODS AND RESULTS

To begin with, let us consider a representative micro heat sink as depicted in Fig. 1 where if a heat flux threshold is passed -the critical heat flux (CHF), a film boiling is formed and the entire surface of the fin is covered by an insulating vapor layer as depicted in Fig. 2. It is desired to know what is the heat transfer between the fin-wall and the bulk liquid.

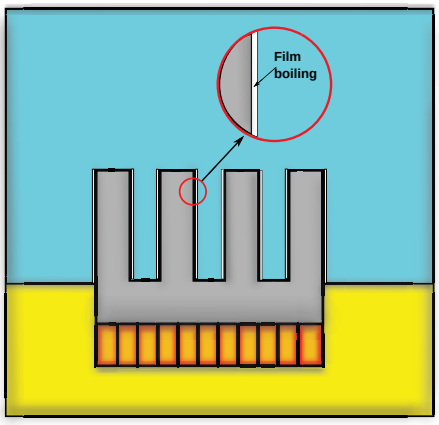

FIG. 2. If the critical heat flux (CHF) is exceeded, an insulating vapor film is formed and covering the entre surface of the fin.

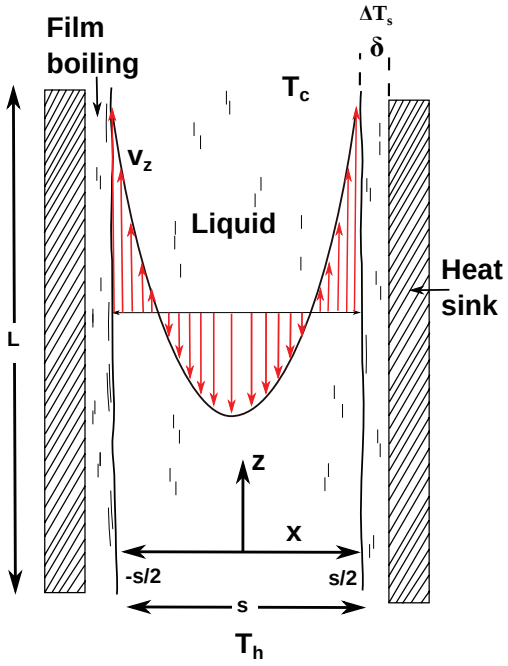

FIG. 3. Physical model of film boiling from a vertical micro heat sink.

- **Momentum consideration**

Let us consider the channel between the micro finned heat sink as depicted in Fig. 3. Let us assume also, that the heat flux through the finned walls is exceeding the critical heat flux (CHF) and as a result a very thin vapor layer or film with thickness δ is formed along the wall. Because the thermal gradient along the vapor film-liquid interface and because the dependence of surface tension with temperature, a surface tension gradient appears which cause that at the interface the liquid flows away from the region of low surface tension (high temperature) toward the region of high surface tension (low temperature). This phenomenon is called Bénard-Marangoni convection, [15].

Vapor inside the film is dragged by the motion of the interface vapor-liquid. On the other hand, the liquid is dragged by the moving interface and the it returns backward causing the appearance of a pressure drop $\frac{dp(z)}{dz}$ along the $z-$axis. With this approach the velocity profile induced by the motion of the interface is given by, [16]

$$v_z = a + bx + \frac{1}{2\mu}\frac{dp(z)}{dz}x^2 \qquad (1)$$

where a and b are constant to be determined by the boundary conditions. If the co-ordinate axes are fixed at the center of the channel and because the symmetry condition (see Fig. 3) it is necessary that $v_z(x) = v(-x)$, an thus $b = 0$ and Eq.(1) becomes

$$v_z = a + \frac{1}{2\mu}\frac{dp(z)}{dz}x^2 \qquad (2)$$

In addition, because the average velocity over the gap cross section equals zero (convective loop)

$$\frac{1}{s}\int_{-\frac{s}{2}}^{\frac{s}{2}} v_z dx = 0 \qquad (3)$$

where it was considered that the thickness of the film can be neglected in comparison with the spacing fin. Inserting Eq.(2) into Eq.(3) and solving yields

$$v_z = \frac{v_i}{2}\left[\frac{12x^2}{s^2} - 1\right] \qquad (4)$$

where v_i is the interface velocity, i.e., $v_z(\frac{s}{2}) = v_z(-\frac{s}{2}) = v_i$

This velocity can be found by equating the viscous-stress tensor with the Marangoni stress at the interface

$$\mu\frac{dv_z}{dx} = -\frac{\partial\sigma}{\partial z} \quad at \quad x = -\frac{s}{2} \qquad (5)$$

or

$$\mu\frac{dv_z}{dx} = \frac{\partial\sigma}{\partial z} \quad at \quad x = \frac{s}{2} \qquad (6)$$

where σ is the surface tension. Applying Eq.(6) or Eq.(5) into Eq.(4) one obtains

$$v_i = \frac{s}{6\mu}\frac{\partial\sigma}{\partial z} \qquad (7)$$

• **Continuity**

The mass flow inside the film is given by

$$\dot{m} = \rho_v \bar{v} w \delta \tag{8}$$

where ρ_v is the density of vapor; $\bar{v}$ the mean velocity inside the film; δ and w the film thickness and the width of the fin, respectively. Because the film is very thin, the the mean velocity ,$\bar{v}$, can be approximated to a linear profile, and then is given by

$$\bar{v} \approx \frac{v_i}{2} \tag{9}$$

and Eq.(8) becomes

$$\dot{m} = \frac{\rho_v v_i w \delta}{2} \tag{10}$$

Finally, the heat flux q transported by the mass flow by the change of phase is given by

$$q = \dot{m} \Delta h$$

$$q = \frac{\rho_v \Delta h v_i w \delta}{2} \tag{11}$$

where Δh is the average enthalpy difference between the vapor and liquid.

• **Heat transfer**

The heat flux is given by

$$q = \frac{\kappa}{\delta} w L \Delta T_s \tag{12}$$

where κ is the liquid thermal conductivity; L the length of the fin; and ΔT_s the superheat or difference of temperature between the wall and the liquid. Equating Eq.(12) with Eq.(11), and solving for the thickness of the film yields

$$\delta = \sqrt{\frac{2\kappa L \Delta T_s}{\rho_v \Delta h v_i}} \tag{13}$$

A heat transfer coefficient may be defined by applying the following equation

$$h = \frac{\kappa}{\delta} \tag{14}$$

Inserting Eq.(13) into Eq.(14) yields

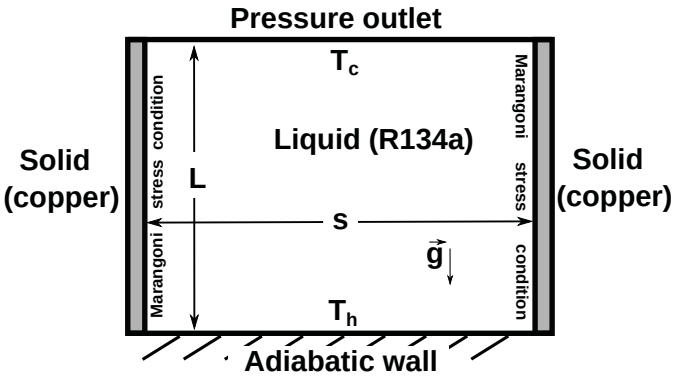

FIG. 4. Schematic of computational simulation setup.

$$h = \sqrt{\frac{\kappa \rho_v \Delta h}{2 L \Delta T_s}} \cdot \sqrt{v_i} \tag{15}$$

considering the expression for the interface velocity driven by Bénard-Marangoni convection, v_i given by Eq.(7), Eq.(15) yields

$$h = \sqrt{\frac{\kappa \rho_v \Delta h s}{12 \mu L \Delta T_s} \frac{\partial \sigma}{\partial z}} \tag{16}$$

Finally, the gradient of surface tension comes from a thermal gradient and then is given by $\frac{\partial \sigma}{\partial z} = \sigma_T \nabla_z T$ being σ_T the surface tension temperature coefficient, and $\nabla_z T$ is the thermal gradient along the interface. This thermal gradient is proportional to $\nabla_z T \sim \frac{T_h - T_c}{L}$ and then Eq.(16) becomes

$$h \approx \frac{\sqrt{s}}{L} \sqrt{\frac{\kappa \rho_v \Delta h \sigma_T (T_h - T_c)}{12 \mu \Delta T_s}} \tag{17}$$

• **Discussion**

It is interesting to see that the film boiling heat transfer is, according with Eq.(15), driven by the interfacial velocities v_i and more precisely $\sqrt{v_i}$. Therefore, a first assessment of the role Bénard-Marangoni convection inn comparison with natural convection can be performed by comparing their typical velocities. The typical fluid velocity v_z driven by natural convection is given by $v_z \sim \frac{g \rho_o \beta (T_h - T_c) s^2}{\mu}$ where g is gravity; ρ_o the liquid density; β the coefficient of thermal expansion; T_h and T_c the hot and cold temperature, respectively; s the

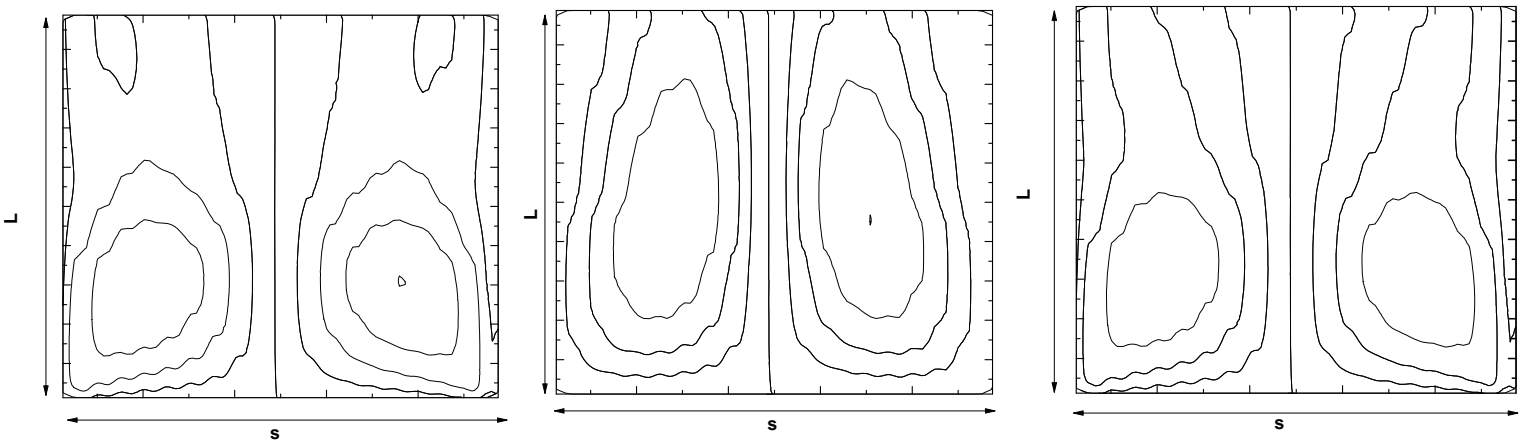

FIG. 5. Streamlines contour. Left: Only Bénard-Marangoni convection. Center: Only natural convection. Right: Mixed convection.

fin spacing; and μ the dynamic viscosity. On the other hand, the Bénard-Marangoni velocity was derived in Eq.(7) which is around $v_z \sim \frac{s\sigma_T(T_h-T_c)}{L\mu}$ where σ_T is the surface tension temperature coefficient and L the length of the fin. It is seen that for micro heat sinks, where the spacing s could be a few millimeters or less, Bénard-Marangoni motion could be comparatively more important.

III. COMPUTATIONAL MODEL

The role of Bénard-Marangoni convection in film boiling heat transfer from micro heat sinks can be assessed by comparing the heat transfer coefficient. Unfortunately, the current state-of-the-art in c Computational Fluid Dynamics (CFD) as regard boiling is almost in an infancy state, and nowadays CFD boiling simulations are restricted to the introduction -by the user, of the second phase and then is not suitable for a direct assesmente of boiling heat transfer process. However, because this work is not intended to typify estimates but rather to asses qualitatively the role of Bénard-Marangoni convection in comparison with natural convection for film boiling heat transfer from micro heat sinks , then it is sufficient to asses the velocity at the interface induced by Bénard-Marangoni convection and natural convection. At this point, from our previous heat transfer analysis, it is seen, from Eq.(15), that the most important parameter is the interfacial velocity v_i and more precisely on $\sqrt{v_i}$ which is easy to convey considering that the interfacial velocity is which is determining the average velocity inside the film and transporting an energy proportional to the phase change enthalpy Δh.

• Problem description:

The problem to be considered is shown schematically in Fig. 4. Coolant R134a was considered inside a rectangular box of sides $s = 1$ mm and $l = 2$mm. The boundary conditions were as follows: at the bottom an adiabatic wall with a constant hot temperature T_h; at the top a pressure outlet condition with a cold temperature T_c; left and right sides as solids with a thickness 0.1mm and made of copper through which heat is transmitted from the bottom wall.
In order to isolate and evaluate separately the role of Bénard-Marangoni and natural convection, the momentum boundary conditions in the fin where adjusted as follows: to isolate the Bénard-Marangoni motion in the left and right sides the option Marangoni stress -available in fluent, was activated and the volumetric expansion coefficient of the fluid was set to zero to prevent buoyancy. To isolate natural convection (without Bénard-Marangoni convection) the left and right sides were fixed with a zero slip condition which more or less simulate the effect of a vapor film and the volumetric expansion coefficient of the liquid was introduced ($\beta = 3.2\times^{-3}$/K). The data for the thermophysical properties of R134a was obtained from Park et.al,2019, [13] and are summarized in table. I.

IV. RESULTS

Fig. 5 shows the comparative stream contours from: Left: Only Bénard-Marangoni convection. Center: Only natural convection. Right: Mixed convection. It is easy to see, that Bénard-Marangoni convection overcomes the effect of natural convection and then is clearly the driven mechanism. Fig. 6 shows the temperature profile for

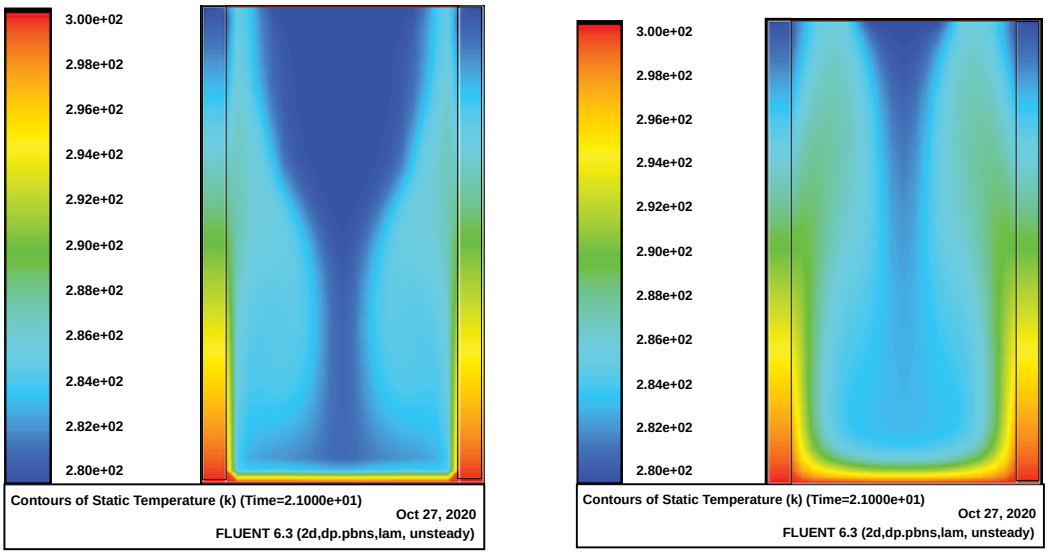

FIG. 6. Contours of temperature. Only Bénard-Marangoni convection. Right: Only natural convection

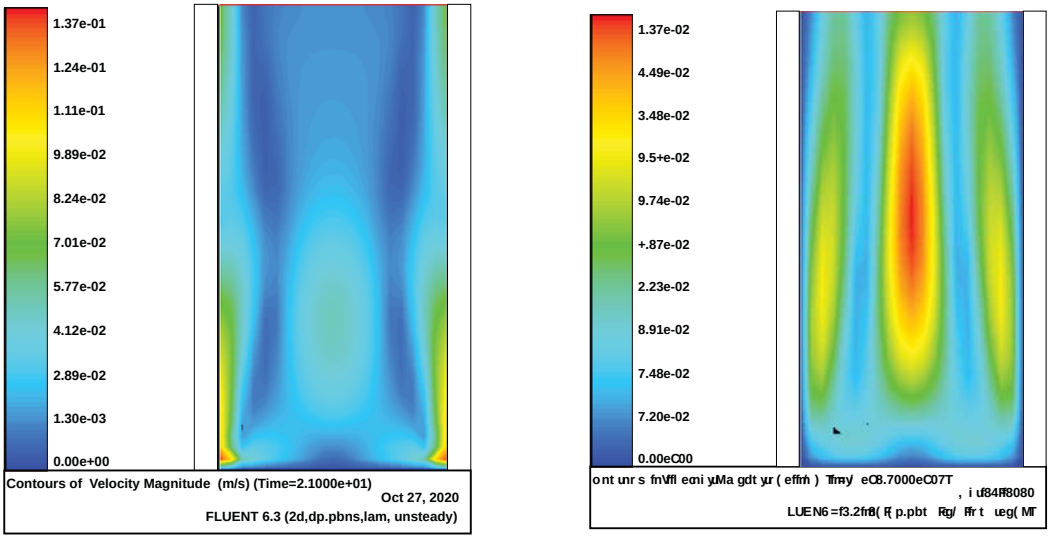

FIG. 7. Contours of velocity. Only Bénard-Marangoni convection. Right: Only natural convection

the isolated effect of Bénard-Marangoni and natural convection, respectively. Finally, Fig. 7 shows the velocity profile for the isolated effect of Bénard-Marangoni and natural convection, respectively, where it is seen that the interfacial velocity at the fins are ar least one order of magnitude higher for Bénard-Marangoni convection, and then it is expected that the heat transfer coefficient ($h \sim \sqrt{v_i}$, from Eq.(15)) will be around 2-to-3 fold than from natural convection.

V. SUMMARY AND CONCLUSIONS

Bénard-Marangoni convection and its significance with regard to film boiling heat transfer from micro heat sinks was discussed. It was found that owing for micro heat sinks the film boiling heat transfer is driven by Bénard-Marangoni convection rather than natural convection. The interfacial velocity induced by Marangoni stress overcomes clearly the induced by natural convection around one order of magnitude higher. Utilizing a simplified physical model, an analytical expression for the film boiling heat transfer coefficient was derived. Because the film boiling heat transfer coefficient is proportional to the interfacial velocity it is expected that the heat transfer coefficient driven by Bénard-Marangoni convection be around 2-to-3- fold than from natural convection. The result encourage further experimental investigation of the subject.

NOMENCLATURE:

a = constant

TABLE I. Thermophysical properties of coolant R134a.¡, from Park eta la, 2019, [13]

	R134a	
	Liquid	Vapor
Density (kg/m^3)	1200	34.19
Thermal conductivity(W/mK)	0.080	0.014
Viscosity(μPas)	190.46	11.77
Latent heat (kJ/kg)	176.08	
Specific heat (kJ/kgK)	1.43	1.04
Surface tension (N/m)	7.8×10^{-3}	
Surface tension coeff. (N/mK)[a]	-0.117×10^{-3}	
thermal expansion coeff (1/K)	3.2×10^{-3}[b]	
Boiling point (K)	300[c]	

[a] [14]
[b] at 298 K
[c] at 1 atm

b = constant
g = gravity
h = heat transfer coefficient
Δh = average enthalpy
L = length of the fin
$\dot{m}$ = mass flow of vapor inside the film
p = pressure
s = fin spacing
T = temperature
ΔT_s = superheat
v_z liquid velocity in z-direction
v_i vapor-liquid interface velocity
$\bar{v}$ mean velocity of vapor
w = width of the fin
x = perpendicular co-ordinate
z = length co-ordinate

Greek symbols

β coefficient of thermal expansion
δ = vapor film thickness
κ = thermal conductivity of liquid
μ = dynamic viscosity
ρ = density of liquid
ρ_v = density of vapor
σ = surface tension
σ_T = surface tension temperature coefficient

subscripts

v = vapor
l = liquid

ACKNOWLEDGEMENTS:

This research was supported by the Spanish Ministry of Economy and Competitiveness under fellowship grant Ramon y Cajal: RYC-2013-13459.

[1] Miniaturization Technologies. 1991. OTA-TCT-514. NTIS order PB92-150325

[2] Rajalingam A; Shubhankar Chakraborty. 2020. Effect of micro-structures in a microchannel heat sink -A comprehensive study. International Journal of Heat and Mass Transfer, Volume 154, 119617,

[3] Mahmoud S; Al-Dadah R; Aspinwall D.K; Soo S.L; Hemida H. 2011. Effect of micro fin geometry on natural convection heat transfer of horizontal microstructures. Applied Thermal Engineering, 31, 5, p.p. 627-633

[4] Yu Jiao; Jiansheng Wang; Xueling Liu. 2020. Flow field characteristic and heat transfer performance in a channel with miniature square filament. International Journal of Heat and Mass Transfer. Volume 163, 120433

[5] Zeghari K. Zeghari, Louahlia H. 2020. Flat miniature heat pipe with sintered porous wick structure: experimental and mathematical studies, International Journal of Heat and Mass Transfer. Volume 158

[6] Tanya Liu; Marc T. Dunham; Ki Wook Jung; Baoxing Chen; Mehdi Asheghi; Kenneth E. Goodson. 2020. Characterization and thermal modeling of a miniature silicon vapor chamber for die-level heat redistribution. International Journal of Heat and Mass Transfer. Volume 152, 119569

[7] Yildizeli Alperen; Cadirci Sertac. 2020. Multi objective optimization of a micro-channel heat sink through genetic algorithm, International Journal of Heat and Mass Transfer. Volume 146, 118847

[8] Wei-Mon Yan, C.J. Ho, Yu-Ting Tseng, Caiyan Qin, Saman Rashidi. 2020. Numerical study on convective heat transfer of nanofluid in a minichannel heat sink with micro-encapsulated PCM-cooled ceiling. International Journal of Heat and Mass Transfer. Volume 153. 119589

[9] Vahid Hosseinpour; Mohammad Kazemeini; Alimorad Rashidi. 2020. Developing a metamodel based upon the DOE approach for investigating the overall performance of microchannel heat sinks utilizing a variety of internal fins. International Journal of Heat and Mass Transfer. Volume 149, 119219.

[10] Bolin He; Xiaoping Luo; Fan Yu; Jianyang Zhou; Jinxin Zhang. 2020. Flow boiling characteristics in bi-porous minichannel heat sink sintered with copper woven tape. International Journal of Heat and Mass Transfer. Volume 158, 119988.

[11] Jaedeok Seo; Wonjung Kim. 2020. Plant leaf inspired evaporative heat sink with a binary porous structure. International Journal of Heat and Mass Transfer. Volume

160, 120171.

[12] John Mathew; Poh-Seng Lee; Tianqing Wu; Christopher R. Yap. 2020. Comparative Study of the Flow Boiling Performance of the Hybrid Microchannel-Microgap Heat Sink with Conventional Straight Microchannel and Microgap Heat Sinks. International Journal of Heat and Mass Transfer, Volume 156, 119812.

[13] Park, J; Peng L; Choi J. 2019. Critical heat flux limiting the effective cooling performance of two-phase cooling with an interlayer microchannel. Microsyst Technol 25. p.p. 2831-2840

[14] Perry, R.H., Green, D.W.: Perry´s Chemical Engineers Handbook. 7. ed. McGraw-Hill 1998.

[15] Getling, A.V. 1998. Rayleigh-Bénard convection : structures and dynamics (Reprint. ed.). Singapore: World Scientific. ISBN 981-02-2657-8.

[16] Fedosov A.I. 1956. Thermocapillary Motion, Zhurnal Fizicheskoi Khimii, 30, N2, p. 366-373.